
Article:

Loughrey, J, Comyn, TP, Apperley, DC et al. (2 more authors) (2014) Complex thermal expansion properties in a molecular honeycomb lattice. Chemical Communications, 50 (57). 7601 - 7603. ISSN 1359-7345

https://doi.org/10.1039/c4cc02198c

Complex Thermal Expansion Properties in a Molecular Honeycomb Lattice†

Jonathan J. Loughrey[a,b], Tim P. Comyn[c], David C. Apperley[d],
Marc A. Little[a,e] and Malcolm A. Halcrow*[a]

[FeL_3][BF$_4$]$_2$·xH$_2$O (L = 3{5}-(pyrazinyl)-1*H*-pyrazole) shows negative thermal expansion between 150-240 K but positive thermal expansion at 240-300 K, linked to rearrangement of anions and water molecules within pores in the lattice.

Eleven years ago, we reported that [FeL_3][BF$_4$]$_2$·xH$_2$O (**1**; L = 3{5}-(pyrazinyl)-1*H*-pyrazole) contains C_3-symmetric *fac*-[FeL_3]$^{2+}$ centres, associated into a chiral 3D honeycomb array through intermolecular N–H…N hydrogen bonding (Figs. 1 and 2).[1] The lattice pores have an approximate diameter of 5.3 Å, and contain a disordered mixture of one BF$_4^-$ equivalent, and lattice water. The other unique BF$_4^-$ ion is crystallographically ordered, and occupies a C_3-symmetric void in the walls of the honeycomb. We noted in our original study that the unit cell volume of **1** is slightly larger at 150 K than at 300 K,[1] making this potentially a new type of negative thermal expansion (NTE) material.[2] This property is best known in certain transition metal oxide or cyanide materials, and in nanoporous metal-organic framework structures.[3] Most NTE materials contain rigid structural components linked by bonds exhibiting pronounced transverse lattice vibrations, which

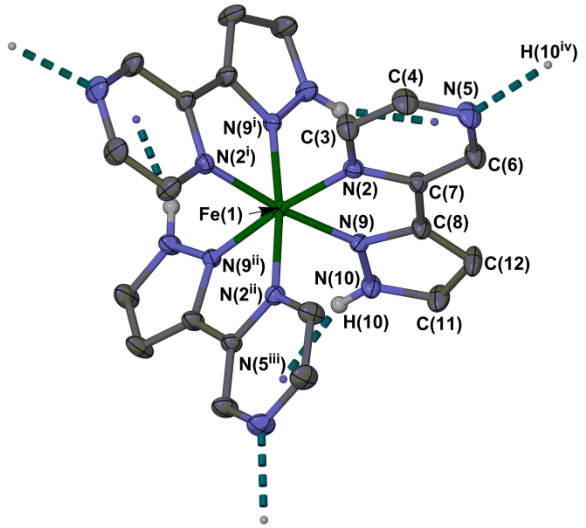

Fig. 1 The [FeL_3]$^{2+}$ dication in **1** at 110 K. Displacement ellipsoids are at the 50 % probability level, and C-bound H atoms are omitted for clarity. Symmetry codes: (i) 1−y, x−y, z; (ii) 1−x+y, 1−x, z; (iii) 1+x−y, 1−y, −½+z; (iv) x−y, 1−y, ½+z.

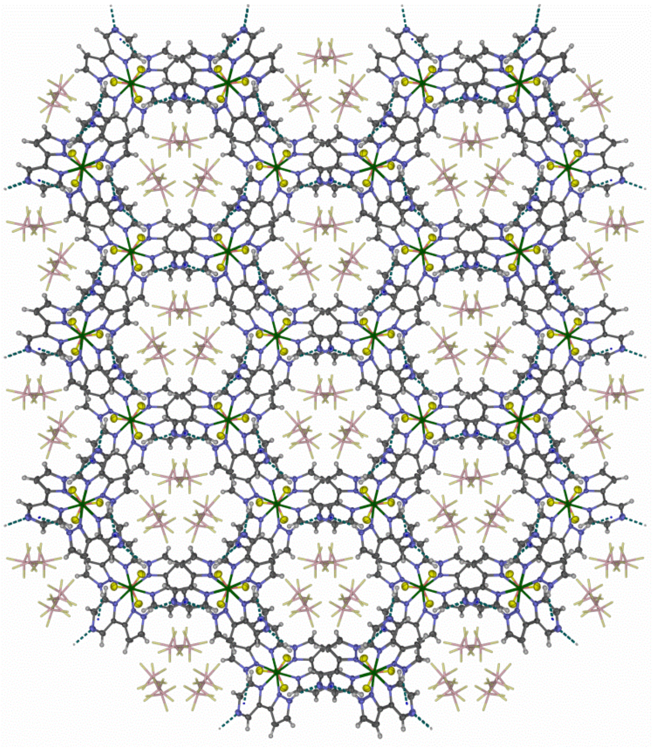

Fig. 2 Packing diagram of **1** at 110 K, showing the channels running parallel to *c*. Displacement ellipsoids are at the 50 % probability level except for the partially occupied disorder sites for the in-channel BF$_4^-$ ions, which are de-emphasised for clarity. Colour code: C, grey; H, pale grey; B, pink; F, yellow; Fe, green; N, blue.

cause canting of the crystal lattice as the sample is warmed.[2] Examples of NTE have also been demonstrated from intermetallic charge transfer in an oxide material[4] and from a conformational change in an organic polymer.[5] NTE in molecular crystals is rarer, but it can arise from changes in intermolecular contacts on cooling,[6] or from the ordering of disordered solvent.[7] We have now reinvestigated the structural chemistry of **1**, and found it to exhibit a more complex thermal expansion behaviour that is linked to its nanoporous structure.

Crystals of **1** are obtained by mixing aqueous solutions of *L* and $Fe[BF_4]_2{\cdot}6H_2O$ in a 3:1 molar ratio, followed by slow evaporation of the resultant mixture. Microanalyses implied a formulation of $[FeL_3][BF_4]_2{\cdot}xH_2O$ with $x \approx 3$. Since our original study described **1** as a dihydrate ($x = 2$),[1] the water content of the pores may vary slightly between samples. TGA analysis of **1** shows only a gradual weight loss on heating (ESI†). There is an inflection point in the TGA curve near 440 K, with a weight loss corresponding to two equivalents of lattice water. Mass loss corresponding to a third water equivalent is not achieved until at least 500 K, where decomposition of the BF_4^- ions can also occur.[8] Loss of water is probably sterically blocked by the in-pore anions, which would account for this high thermal stability.

The crystal structure of **1** was re-investigated, at 300 and 110 K (ESI†). The results are consistent with our initial report ‡,[1] but the higher resolution of the new data allowed the intra-pore anion to be partially refined over one or two unique disorder sites (Fig. 2). The estimated occupancy of these disorder sites varied between experiments, at between 30 and 78 % of the total BF_4^- content of the pores; the higher value was obtained from the low temperature refinement. These partial anion sites form a weak C–H...F contact to the *C*5 position of the pyrazinyl ring in *L* (C...F = 3.3-3.4 Å, ESI†). There are no other noteworthy differences between the refinements at 300 and 110 K; in particular, the pore diameter is almost constant at 5.2 Å (300 K) and 5.4 Å (110 K). *SQUEEZE* analyses[9] based on models lacking the in-pore anion sites implied that the pores contain between 61-79 electrons per complex molecule, which is consistent with the presence of one BF_4^- ion (41 electrons) and 2-4 equivalents of water (10 electrons each).

The low-temperature structure of **1** was only accessible if the crystal was flash-cooled. If the sample is cooled more slowly it becomes twinned below *ca.* 240 K, which sometimes leads to decomposition of the crystal. If the crystals survive the twinning process the transition is reversible, and they become single again on re-warming to room temperature. Such crystals sometimes present the same trigonal unit cell below 240 K‡, or sometimes a monoclinic one, but in each case the structure cannot be properly refined. Structure determinations of **1** at 300 K were indistinguishable before and after cycling across the twinning temperature (ESI†).

Variable temperature unit cell data from single crystals of **1** show some variability and scatter, particularly below 200 K (Fig. 3 and ESI†). Unit cells derived from X-ray powder diffraction data (see below) are more consistent, and show comparable trends to the single crystal parameters (Fig. 3). The unit cell *c* parameter increases continuously on cooling between 290 and 100 K, along the direction of the lattice pores. In contrast *a* decreases on cooling, at a comparable rate to *c*. The volume (*V*) appears to decrease on cooling to a minimum around 240 K before increasing again at lower temperatures, and possibly plateauing near 150 K. The apparent minimum in *V* near 240 K coincides with the crystal twinning event described above. Notably *V* is almost identical at 150 and 300 K by both techniques, in agreement with our original report.[1] The single crystal data in Fig. 3, measured in cooling and warming modes, show there is no measurable hysteresis in the thermal expansion of the crystal.

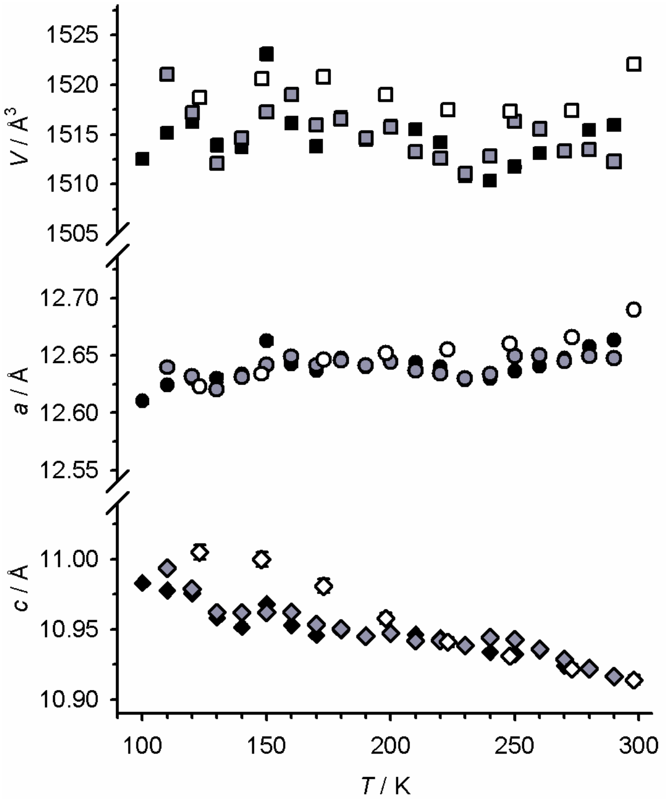

Fig. 3 Variable temperature unit cell data for **1**. Colour code: black, single crystal, cooling mode; grey, single crystal, warming mode; white, powder diffraction. Error bars are shown, but are mostly smaller than the symbols on the graph.

X-ray powder diffraction patterns from **1** show excellent agreement with a simulation from the single crystal phase at low angle (ESI†). However, a few additional reflections appear at higher angle, which might be associated with the pore contents which could not be included in the simulation. The same diffraction pattern was retained between 123 and 300 K, implying the reversible twinning in the single crystal does not reflect any gross structural changes. Gradual and reversible peak broadening was observed below *ca.* 220 K, however, indicating a reduction in the crystallinity of the material (ESI†). That is consistent with the increased errors on the single crystal unit cell parameters at low temperatures.

Although anhydrous $[FeL_3][BF_4]_2$ is unstable under ambient conditions,[1] dehydration of **1** under vacuum was achieved *in situ* on the powder diffractometer, leading to a new lower symmetry crystalline phase (ESI†). This new phase spontaneously reconverts to **1** upon exposure to air, however, and no further characterisation of the anhydrous material was achieved.

The role of the anions in the thermal expansion of **1** was probed by solid state ^{11}B and ^{19}F NMR. Both spectra contain two peaks as expected, one of them significantly broader than the other (ESI†).[1] The broader resonances can be assigned to the static framework BF_4^- environment, and the narrower ones to the more dynamic in-pore BF_4^- ions. The framework resonance ^{19}F linewidth shows a linear temperature dependence between 160-300 K. In contrast the ^{19}F linewidth from the in-pore BF_4^- ions decreases on warming between 160-200 K, stays almost constant between 200-260 K, then increases with temperature between 260-300 K (Fig. 4). This implies a change in the dynamics of the pore contents at lower temperatures, concomitant with the switch from negative to positive thermal volume expansion (Fig. 3). This change in dynamics does not occur abruptly, as would be expected for a crystallographic phase transition. Rather, its gradual onset is consistent with the disordered nature of the pore contents. The same ^{19}F linewidth trends were observed upon rewarming the sample after rapidly quenching it to 168 K (Fig. 4).

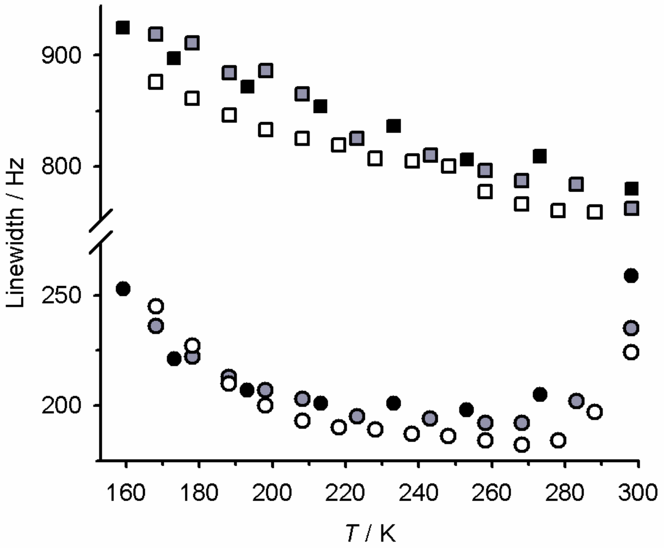

Fig. 4 ^{19}F NMR linewidths for the in-pore (circles) and framework (squares) BF_4^- ions. Data were measured using the following temperature ramps: slow cool (black); slow rewarm (grey); and rapid quench then rewarm (white).

In conclusion, the honeycomb lattice **1** exhibits complex thermal expansion properties, which reflect a balance between uniaxial NTE in *c*, along the direction of the lattice pores, and more usual positive thermal expansion (PTE) behaviour in *a* (perpendicular to the pore direction). This leads to an apparent inversion in its thermal volume expansion near 240 K, which is associated with a reversible twinning transition that substantially stresses the crystal lattice. The twinning event does not cause significant changes to the framework structure, but is linked to the dynamics of the pore contents. To our knowledge, the closest literature analogue to **1** is the dipeptide TrpGly·H_2O, which exhibits uniaxial NTE along helical water channels in the lattice. This was proposed to originate from a gradual ordering of the lattice water as the temperature is lowered.[7] A comparable rearrangement of the pore contents in **1** is probably responsible for its unusual thermal properties.

This work was funded by the University of Leeds. Solid-state NMR spectra were obtained at the EPSRC UK National Solid-state NMR Service at Durham. The authors also thank Dr H.J. Shepherd for help with the single crystal unit cell measurements.

Notes and references

[a] *School of Chemistry, University of Leeds, Leeds, UK LS2 9JT. E-mail: m.a.halcrow@leeds.ac.uk; Fax: +44 113 343 6565; Tel: +44 113 343 6506.*
[b] *Current address: Department of Chemistry and Biochemistry, University of Arizona, P.O. Box 210041, 1306 East University Blvd., Tucson, AZ 85721-0041, USA*
[c] *Institute for Materials Research, School of Process, Environmental and Materials Engineering, University of Leeds, Leeds, UK LS2 9JT.*
[d] *EPSRC Solid State NMR Service, Department of Chemistry, University of Durham, South Road, Durham, UK DH1 3LE.*
[e] *Current address: Department of Chemistry, University of Liverpool, Crown Street, Liverpool, UK L69 7ZD*

† Electronic Supplementary Information (ESI) available: Experimental details, additional Figures and Tables. CCDC 992761−992764. For ESI see DOI: 10.1039/####.

‡ The space group of **1** is *P*31*c*, which was erroneously written as $P3_1/c$ in ref. 1.

1 R. J. Smithson, C. A. Kilner, A. R. Brough and M. A. Halcrow, *Polyhedron*, 2003, **22**, 725.
2 J. S. O. Evans, *J. Chem. Soc*., *Dalton Trans*., 1999, 3317; W. Miller, C. W. Smith, D. S. Mackenzie and K. E. Evans, *J. Mater. Sci*., 2009, **44**, 5441; C. Lind, *Materials*, 2012, **5**, 1125.
3 A. B. Cairns and A. L. Goodwin, *Chem. Soc. Rev.*, 2013, **42**, 4881.
4 M. Azuma, W. Chen, H. Seki, M. Czapski, S. Olga, K. Oka, M. Mizumaki, T. Watanuki, N. Ishimatsu, N. Kawamura, S. Ishiwata, M. G. Tucker, Y. Shimakawa and J. P. Attfield, *Nature Comm.*, 2011, **2**, 347.
5 X. Shen, C. Viney, E. R. Johnson, C. Wang and J. Q. Lu, *Nature Chem.*, 2013, **5**, 1035.
6 D. Das, T. Jacobs and L. J. Barbour, *Nature Mater.*, 2010, **9**, 36; S. Smeets and M. Lutz, *Acta Cryst., Sect. C Cryst. Struct. Commun.*, 2011, **67**, m50; S. Bhattacharya and B. K. Saha, *Cryst. Growth Des.*, 2012, **12**, 4716; R. H. Jones, K. S. Knight, W. G. Marshall, J. Clews, R. J. Darton, D. Pyatt, S. J. Coles and P. N. Horton, *CrystEngComm*, 2014, **16**, 237; E. R. Engel, V. J. Smith, C. X. Bezuidenhout and L. J. Barbour, *Chem. Commun.*, 2014, **50**, 4238.
7 H. Birkedal, D. Schwarzenbach and P. Pattison, *Angew. Chem., Int. Ed.*, 2002, **41**, 754; Y. Pan, H. Birkedal, P. Pattison, D. Brown and G. Chapuis, *J. Phys. Chem. B*, 2004, **108**, 6458.
8 D. Göbbels and G. Meyer, *Z. Anorg. Allg. Chem.*, 2002, **628**, 1799.
9 A. L. Spek, *J. Appl. Cryst.*, 2003, **36**, 7.